Fate of Volatile Organic Compounds in Constructed Wastewater Treatment Wetlands

STEFFANIE H. KEEFE,[†]
LARRY B. BARBER,*,[†]
ROBERT L. RUNKEL,[‡] AND
JOSEPH N. RYAN[§]

U.S. Geological Survey, 3215 Marine Street, Room E127, Boulder, Colorado 80303, Denver Federal Center, P.O. Box 25046, Mail Stop 415, Lakewood, Colorado 80225, and University of Colorado, 428 UCB, Boulder, Colorado 80309

The fate of volatile organic compounds was evaluated in a wastewater-dependent constructed wetland near Phoenix, AZ, using field measurements and solute transport modeling. Numerically based volatilization rates were determined using inverse modeling techniques and hydraulic parameters established by sodium bromide tracer experiments. Theoretical volatilization rates were calculated from the two-film method incorporating physicochemical properties and environmental conditions. Additional analyses were conducted using graphically determined volatilization rates based on field measurements. Transport (with first-order removal) simulations were performed using a range of volatilization rates and were evaluated with respect to field concentrations. The inverse and two-film reactive transport simulations demonstrated excellent agreement with measured concentrations for 1,4-dichlorobenzene, tetrachloroethene, dichloromethane, and trichloromethane and fair agreement for dibromochloromethane, bromo-dichloromethane, and toluene. Wetland removal efficiencies from inlet to outlet ranged from 63% to 87% for target compounds.

Introduction

Constructed wetlands are a treatment alternative used to improve the quality of municipal and industrial wastewater effluents, agricultural and livestock operation runoff, and nonpoint-source pollution including pesticides and acid mine drainage (*1–6*). The primary transformation pathways affecting the fate of trace organic compounds in aquatic systems such as treatment wetlands include sorption, biotransformation, photolysis, and volatilization (*7*). Low levels of volatile organic compounds (VOC) can persist in municipal wastewater effluents and are of concern when released into aquatic environments (*8*). Chlorination of wastewater effluents can produce a variety of chlorinated and brominated VOC (*9*). Surface-water constructed wetlands are typically designed with large surface areas and alternating deep and shallow zones, which increase solute contact with the air–water interface, promoting VOC removal. Many wetland studies have focused on long-term mass balance measurements of inlet and outlet concentrations of biochemical oxygen demand, ammonia, suspended solids, nitrogen, and phosphate (*10–14*). Fewer studies have focused on the behavior of organic compounds (*2, 15–17*), and less work has been done on the fate of VOC in treatment wetlands (*18–21*).

Deterministic, steady-state models have been used to define kinetic rates based on first-order areal or volumetric removal rates without focus on internal removal functions (*5, 22–24*). Kadlec (*25*) noted the inadequacy of first-order models at incorporating the strong correlation of removal rates to hydraulic loading rate (HLR, volumetric flow rate divided by surface area; *5*) and initial concentration. Buchberger and Shaw (*26*) represented reactive transport in constructed wetlands as a combination of nonideal plug flow reactors and first-order decay rates. These techniques illustrate the limitations of current research in linking wetland hydraulics to removal pathways.

In this paper, we discuss the transport and volatilization of VOC in a constructed wetland that receives secondary-advanced, activated-sludge treated denitrified, chlorinated municipal wastewater. Tracer test data were used to quantify wetland hydrodynamics describing main channel transport and associated transient storage interactions (*27*). VOC removal was simulated using the OTIS (one-dimensional transport with inflow and storage) solute transport model (*28*) with inverse, theoretical, and graphical volatilization rates. The simulations are presented as a means of quantifying physical and chemical processes and to introduce a technique for investigating reactive transport in constructed wetlands.

Methods

Site Description. The experiment was conducted at the Tres Rios Demonstration Wetlands (*29*), located near the Salt River in Maricopa County, southwest of Phoenix, AZ. The wetlands were constructed in 1995 to process effluent from the City of Phoenix 91st Avenue Wastewater Treatment Plant (WWTP). The site consists of four individual 0.90–1.34-ha wetlands that collectively receive 3780 m³ s⁻¹ (1.0 MGD) of secondary-advanced treated municipal wastewater (*30*). The Hayfield 1 (H1) wetland (Figure 1) was constructed on a former agricultural field consisting of topsoil that curtails groundwater seepage and has five internal sinusoidal deep zones (1.5 m depth) alternating with shallow emergent vegetated zones (0.5 m depth). Wetland flow was controlled through 60° v-notched inlet and outlet weirs. In June 1999, the H1 wetland contained ~30% emergent vegetation consisting of softstem bulrush (*Schoenoplectus tabernaemontani*) and Olney's bulrush (*Schoenoplectus americanus*) as well as duckweed (*Lemna* spp.) growth on the deep zone water surface (Table 1). The HLR was 15 cm d⁻¹.

Field Sampling. Water samples were collected at the inlet splitter box, in each deep zone, and at the wetland outlet of the H1 wetland on February 16, 2000, for determination of VOC (Figure 1). Quadruplicate water samples were collected in 40-mL amber glass bottles. The bottles were submerged to the midpoint of the water column and filled with no headspace to prevent volatilization losses, preserved by the addition of 0.5 mL of hydrochloric acid and 250 mg of ascorbic acid, and stored at 4 °C until analysis. Water temperature was 24.6 °C at the Hayfield inlet splitter box. Hourly wind speed velocities were obtained 3 m above the ground from the Arizona Meteorological Network Litchfield weather gauging station located approximately 30 km away (http://ag.arizona.edu/azmet/). The wind velocities averaged 1.2 m s⁻¹ with a range of 0.4–1.9 m s⁻¹ on February 16, 2000.

* Corresponding author phone: (303)541-3039; fax: (303)447-2505; e-mail: lbbarber@usgs.gov.
[†] U.S. Geological Survey.
[‡] Denver Federal Center.
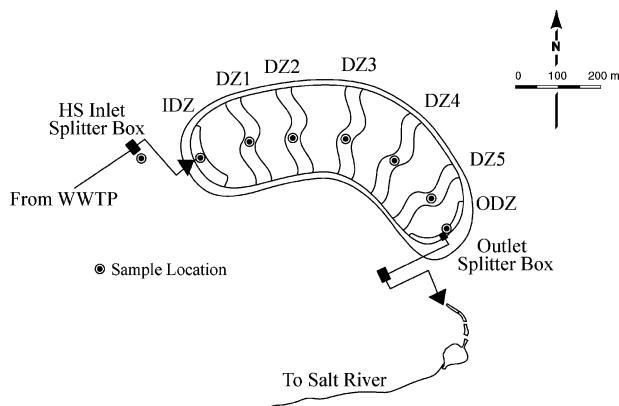[§] University of Colorado.

FIGURE 1. Hayfield 1 wetland (DZ = deep zone, HS = Hayfield site, I = inlet, O = outlet, WWTP = wastewater treatment plant).

Laboratory Analysis. Water samples were analyzed for VOC (*31*) by the U.S. Geological Survey National Water Quality Laboratory (NWQL). The inlet splitter box sample was analyzed using NWQL Schedule 2020 (86 compounds), and the remainder of internal wetland samples were analyzed using Schedule 2022 (34 compounds). A Tekmar model LSC 2000 concentrator with a Tekmar Aquatek automatic purge-and-trap unit was used to bubble helium through a 25-mL aliquot of the environmental sample. A VOCARB 3000 trap containing 10 cm of (60/80 mesh) Carbopak B (Supelco), 6 cm (60/80) Carboxen mesh, and 1 cm of (60/80 mesh) Carboxen 1001 were used to trap the VOC. Compounds were thermally desorbed into a Megabore (J&W DB-624, 75 m × 0.53 mm i.d.) capillary gas chromatography column interfaced with a Hewlett-Packard model 5971/5972 gas chromatograph/mass spectrometer (subambient oven-cooling, jet separator). The VOC were identified using standard reference materials and comparing retention times and relative ion ratios of the mass spectra.

Modeling

Solute Transport. The physical and chemical processes governing solute transport and volatilization in the wetland were quantified using measured field data and the OTIS model (*28*). OTIS has been used extensively in stream and river systems (*32–34*), but only recently has it been applied to quantify the effects of transient storage on conservative and reactive transport in constructed wetlands (*27, 35*). For this application, the concentrations of reactive (volatile) compounds are assumed to be relatively steady state over long time periods. On shorter time scales, however, WWTP effluents have diel variations in content resulting from daily fluctuations of influent composition. The governing equation for the main channel at steady state is therefore (*28*):

$$0 = -\frac{Q}{A}\frac{\partial C}{\partial x} + \frac{1}{A}\frac{\partial}{\partial x}\left(AD\frac{\partial C}{\partial x}\right) + \frac{q_{evap}}{A}C - k_{vol}C \qquad (1)$$

where Q is volumetric flow rate (m³ s⁻¹), A is main channel cross-sectional area (m²), C is concentration in the main channel (μg L⁻¹), x is distance (m), D is longitudinal dispersion coefficient (m² s⁻¹), q_{evap} is rate of evaporation (m³ s⁻¹ m⁻¹), and k_{vol} is volatilization rate coefficient for the main channel (s⁻¹).

Conservative Transport. A sodium bromide tracer experiment was conducted in the H1 wetland during June to July 1999, 7 months prior to the VOC field survey. The operational conditions of the 1999 tracer experiment are given in Table 1. The H1 wetland had 30-cm shallow zone depths and about 30% vegetation coverage during both the June 1999 and February 2000 field experiments. The hydrologic

TABLE 1. Hydraulic and Transient Storage Parameters for the Hayfield 1 Wetland Bromide Tracer Test, June to July 1999 (*27*)[a]

Physical	
basin length (m)	228
basin width (m)	60
no. of deep zones	5
no. of shallow zones	6
shallow zone depth (cm)	30
bulrush (%)	30
Measured	
Q_{in} (m³ s⁻¹)	2.19×10^{-2}
Q_{out} (m³ s⁻¹)	1.70×10^{-2}
Q_{evap} (m³ s⁻¹)	1.52×10^{-3}
Q_{inf} (m³ s⁻¹)	3.34×10^{-3}
design volume (m³)	6760
HLR (cm d⁻¹)	15
HRT (d)	3.89
Modeled	
A (m²)	24.2 ($\pm$ 0.21)
D (m² s⁻¹)	9.97×10^{-3} ($\pm 2.35 \times 10^{-4}$)
A_s (m²)	3.90 ($\pm$ 0.26)
α (s⁻¹)	9.00×10^{-7} ($\pm 1.35 \times 10^{-7}$)

[a] Q_{in} = average daily volumetric inflow rate; Q_{out} = average daily volumetric outflow rate; Q_{evap} = average daily evaporation volumetric flow rate; Q_{inf} = average daily infiltration volumetric flow rate; HLR = hydraulic loading rate; HRT = hydraulic retention time; A = main channel cross-sectional area; D = longitudinal dispersion coefficient; A_s = storage zone cross-sectional area; α = storage zone exchange coefficient. Values in parentheses represent parameter standard deviation.
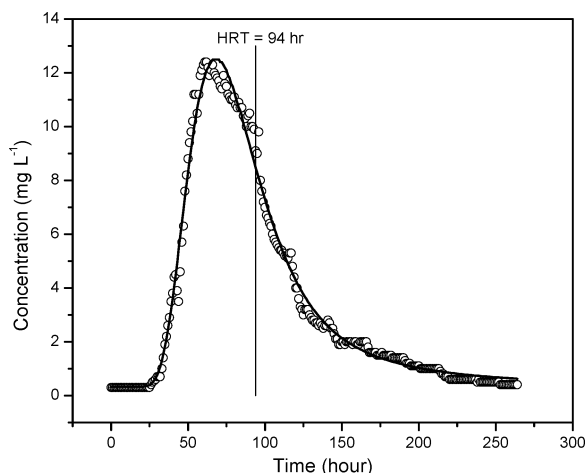

FIGURE 2. Bromide tracer test breakthrough curve and OTIS model simulation for the Hayfield 1 wetland, June 24–July 6, 1999 (*27*) (HRT = hydraulic retention time)

conditions during the VOC field survey differed slightly from the H1 bromide tracer test with the winter season having a 0.94-cm (10%) difference in reference evapotranspiration relative to the mid-summer conditions. Although, conservative transport parameters (Table 1) directly depend on the amount of water present in the system, it is assumed that the difference between the water budgets of the two sampling events did not substantially influence the transport characteristics. Therefore, the bromide tracer test results and the steady, nonuniform water budget provide a basis to describe the hydrologic conditions during the VOC sampling. The bromide tracer test breakthrough curve (Figure 2) was used to quantify the physical processes affecting solute transport in the wetland, and the resulting conservative transport parameters were estimated by comparing transport simulations with measured tracer data (Table 1). Details of the parameter estimation techniques are presented elsewhere (*27*).

TABLE 2. Molecular Weight (m), Molar Volume ($\bar{V}$), Henry's Law Coefficient (K_H), Inlet Deep Zone Concentration (C_{in}), Laboratory Reporting Limit for Long-Term Method Variability, Percent Removal at the Outlet, and Mass Flux to the Atmosphere of VOC Detected in the Hayfield 1 Field Sampling on February 16, 2000

compound	m (g mol⁻¹)	$\bar{V}$ᵃ (cm³ mol⁻¹)	K_Hᵇ (atm L mol⁻¹)	C_{in} (μg L⁻¹)	lab reporting limit (μg L⁻¹)	removal at outlet (%)ᶜ	atmos flux (g d⁻¹ ha⁻¹)
			Target VOC				
bromodichloromethane	163.8	94.7	2.12	2.16	0.05	83.4	2.47
dibromochloromethane	208.3	97.1	0.78	0.77	0.18	86.5	0.91
1,4-dichlorobenzene	147.0	132.5	2.40	0.74	0.05	65.5	0.69
dichloromethane	84.9	71.4	3.25	0.87	0.38	63.3	0.78
tetrachloroethene	165.8	128.0	17.70	0.48	0.10	65.4	0.45
trichloromethane	119.4	92.3	3.67	4.45	0.05	66.4	4.19
toluene	198.5	186.7	6.64	0.23	0.05	63.4	0.21
			Low-Level VOCᵈ				
benzene	78.1	90.7	5.55	0.01	0.04	31.1	0.01
chlorobenzene	112.6	111.6	3.77	0.03	0.03		0.04
diethyl ether	74.1	103.6	1.23	0.10	0.17	37.1	0.06
ethylbenzene	106.2	135.1	7.88	0.01	0.03		0.01
methyl-*tert*-butyl ether	88.2	125.8	0.59	0.13	0.17	39.8	0.08
trichloroethene	131.4	107.1	9.85	0.07	0.04	58.9	0.06
1,2-xylene	106.2	135.1	5.18	0.02	0.04	39.3	0.01
1,3- + 1,4-xylene	106.2	135.1	7.18	0.02	0.06	20.8	0.01

ᵃ LeBas molar volume (39). ᵇ Measured Henry's law coefficient (K_H) (40). ᶜ Removal (%) calculated as $(C_{in} - C_{out})/C_{in} \times 100$. ᵈ Compounds detected at concentrations near or below laboratory reporting level.

Reactive Transport. Solute transport within the wetland results in significant contact with the air−water interface promoting volatilization reactions. Reactive simulations were therefore conducted using OTIS to quantify the effects of first-order volatilization on VOC transport using the physical transport parameters estimated from the bromide tracer data and inverse, two-film, and graphically determined volatilization rates.

VOC Mass Balance. Mass removal (% removal) within the wetland was calculated for each VOC as $100(C_{in} - C_{out})/C_{in}$ where C_{in} is inlet deep zone (IDZ) concentration (μg L⁻¹) and C_{out} is outlet deep zone (ODZ) concentration (μg L⁻¹). VOC mass flux to the atmosphere was calculated as the difference between the mass loading rate and the export rate corrected for mass and flow loss (11%) to groundwater infiltration. VOC mass loading and export rates (g d⁻¹ ha⁻¹) were calculated as VOC mass in $(86.4Q_{in}C_{in})$ and mass out $(86.4Q_{out}C_{out})$ normalized to wetland surface area (1.34 ha), where Q_{in} is the average daily volumetric inflow rate (m³ s⁻¹) and Q_{out} is the average daily volumetric outflow rate (m³ s⁻¹).

Inverse Reactive Simulations. Inverse modeling simulations were conducted to calculate volatilization rates ($k_{vol,inverse}$) from field VOC measurements. Parameter estimation to determine first-order removal rates producing the closest correspondence between simulated and observed concentrations was facilitated by OTIS-P, a nonlinear least squares approach to minimize differences between simulated and observed concentrations (28). Corresponding inverse half-life values, ($t_{1/2,inverse}$) were calculated from $\ln(2)/k_{vol,inverse}$, which includes a 95% confidence interval as a measure of parameter regression variability.

Two-Film Reactive Simulations. The two-film theory of volatilization was used to mathematically describe molecular diffusion across laminar aqueous and gas boundary layers at the water surface (7, 36−38). The two-film first-order volatilization rate coefficient, $k_{vol,2-film}$, was calculated by distributing the overall rate of transfer of a compound through both boundary layers, k_{wo} (cm s⁻¹), over the entire depth of the water column, Y (cm) (7):

$$k_{vol,2-film} = \frac{k_{wo}}{Y} = \frac{1}{Y}\left[\frac{RT}{K_H V_{a,comp}} + \frac{1}{v_{w,comp}}\right]^{-1} \quad (2)$$

The k_{wo} parameter is a function of transfer velocity through the air layer, $v_{a,comp}$ (cm s⁻¹), and transfer velocity through the water boundary layer, $v_{w,comp}$ (cm s⁻¹). The rate of mass transfer through the air layer is influenced by the ideal gas constant, R (0.082 atm L mol⁻¹ K⁻¹), temperature, T (K), and the compounds Henry's law constant, K_H (atm L mol⁻¹). Table 2 lists the relevant physicochemical properties (39, 40) for the VOC detected in the field sampling.

The transfer velocity in the water layer of each compound of interest, $v_{w,comp}$, was calculated as a function of diffusion relative to an oxygen molecule (7):

$$v_{w,comp} = v_{w,oxy}\left[\frac{D_{w,comp}}{D_{w,oxy}}\right]^{0.5} \quad (3)$$

where $v_{w,oxy}$ is the transfer velocity of an oxygen molecule through the water layer (cm s⁻¹), $D_{w,comp}$ is the diffusivity coefficient of a compound of interest in the water layer (cm² s⁻¹), and $D_{w,oxy}$ is the diffusivity coefficient of an oxygen molecule in the water layer (cm² s⁻¹).

The diffusivity coefficient through the water layer (D_w) of an oxygen molecule ($D_{w,oxy}$) and each compound of interest ($D_{w,comp}$) was calculated by (41):

$$D_w = \frac{13.26 \times 10^{-5}}{\mu_w^{1.14}\bar{V}^{0.589}} \quad (4)$$

where μ_w is the water viscosity at temperature T (10⁻² g cm⁻¹ s⁻¹) and $\bar{V}$ is the molar volume (cm³ mol⁻¹).

The $v_{w,oxy}$ parameter depends primarily on the wind velocity (7):

$$v_{w,oxy} = (4 \times 10^{-4}) + (4 \times 10^{-5})\left[\frac{10.4u_z}{\ln(z) + 8.1}\right]^2 \quad (5)$$

where u_z is wind velocity (m s⁻¹) recorded at vertical distance z (m) above the water surface. Increased wind velocity decreases the thickness of the water and air boundary layers, which causes a proportional rise in the rate of volatilization.

The transfer velocity of each compound of interest in the air layer ($v_{a,comp}$) was estimated as a function of diffusion

relative to a water molecule (7):

$$v_{a,comp} = v_{a,H_2O} \left[\frac{D_{a,comp}}{D_{a,H_2O}} \right]^{0.6} \quad (6)$$

where v_{a,H_2O} is the transfer velocity of a water molecule through the air layer (cm s^{-1}), $D_{a,comp}$ is the diffusivity coefficient of the compound of interest in the air layer (cm^2 s^{-1}), and D_{a,H_2O} is the diffusivity coefficient of a water molecule in the air layer (cm^2 s^{-1}).

The diffusivity coefficient in the air layer (D_a) of a water molecule (D_{a,H_2O}) and each compound of interest ($D_{a,comp}$) was calculated by (42):

$$D_a = \frac{(10^{-3})(T^{1.75})\left[\frac{1}{m_{air}} + \frac{1}{m}\right]^{0.5}}{P[\bar{V}_{air}^{1/3} + \bar{V}^{1/3}]^2} \quad (7)$$

where m_{air} is the average molecular mass of air (28.97 g mol^{-1}), m is the compound molecular mass (g mol^{-1}), P is the gas-phase pressure (1 atm), and $\bar{V}_{air}$ is the average molar volume of gases in air (20.1 cm^3 mol^{-1}).

The v_{a,H_2O} parameter depends primarily on the wind velocity (7):

$$v_{a,H_2O} \approx 0.2 \left[\frac{10.4 u_z}{\ln(z) + 8.1} \right] + 0.3 \quad (8)$$

As the average wind speed increases, the gas-film thickness decreases resulting in a faster $v_{a,comp}$ value.

Reactive simulations were performed using $k_{vol,2-film}$ (eq 2) for each VOC in order to evaluate the suitability of theoretically calculated volatilization rates in conjunction with experimentally determined hydraulic transport parameters. Two-film half-lives ($t_{1/2,2-film}$) were calculated from two-film volatilization rates ($k_{vol,2-film}$) independent of wetland hydraulics (i.e., $\ln(2)/k_{vol,2-film}$).

Graphical Reactive Simulations. Reactive simulations were carried out using graphically determined volatilization rates ($k_{vol,graph}$). To calculate $k_{vol,graph}$ for each VOC, field measurements were converted from distance to time using a fractional distance and flow estimate at each sample location. The flow at any location within the wetland (Q_x) was estimated as a linear function of distance:

$$Q_x = Q_{in} - q_{evap}x - q_{inf}x \quad (9)$$

where q_{evap} (Q_{evap}/wetland length) is the rate of evaporation (m^3 s^{-1} m^{-1}), q_{inf} (Q_{inf}/wetland length) is the rate of groundwater infiltration (m^3 s^{-1} m^{-1}), Q_{evap} is the average daily evaporation volumetric flow rate (m^3 s^{-1}), and Q_{inf} is the average daily infiltration volumetric flow rate (m^3 s^{-1}). An average flow ($Q_{avg,x}$) between the inlet and a sample location at a distance x was estimated by $Q_{avg,x} = 0.5(Q_{in} + Q_x)$. A corresponding average velocity ($u_{avg,x}$) was calculated by normalizing flow to the main channel cross-sectional area (A) such as $u_{avg,x} = Q_{avg,x}/A$. Finally, a travel time to each sample location (t_x) was calculated by x/u_{avg}. The graphical approach was used to determine volatilization rates ($k_{vol,graph}$) based on the slope of a $\ln(C/C_o)$ versus travel time plot of VOC field measurements, where C_o is the initial concentration, and associated half-life values ($t_{1/2,graph}$) were calculated based on $\ln(2)/k_{vol,graph}$.

Results

VOC Measurements. Table 2 lists the VOC detected in the H1 wetland. A complete compilation of VOC measurements are presented elsewhere (43). Only 7 of the 34 compounds measured were detected at concentrations substantially

above detection limits and are referred to as target VOC. Laboratory reporting limits (Table 2) represent the long-term variance of multiple instruments, multiple operators, and multiple calibrations over an extended time. From the wetland inlet (IDZ) to the outlet (ODZ), concentrations were substantially reduced (63−87%) for 1,4-dichlorobenzene, tetrachloroethene, dichloromethane, trichloromethane, bromodichloromethane, dibromochloromethane, and toluene. The atmospheric flux of target VOC ranged from 0.21 g d^{-1} ha^{-1} for toluene to 4.19 g d^{-1} ha^{-1} for trichloromethane.

Table 2 also lists VOC detected in field samples at concentrations near detection limits, referred to as low-level VOC. Concentrations were reduced by 21−59% from the IDZ to the ODZ for benzene, diethyl ether, methyl-*tert*-butyl ether, trichloroethene, 1,2-xylene, and 1,3- + 1,4-xylene. Between the IDZ and the third deep zone (DZ3), concentrations of chlorobenzene were reduced by about 68% and ethylbenzene was reduced by 14%. The low-level VOC atmospheric fluxes ranged from 0.01 g d^{-1} ha^{-1} for benzene to 0.08 g d^{-1} ha^{-1} for methyl-*tert*-butyl ether.

Concentration reductions from the inlet splitter box to the IDZ reflect VOC removal as the wastewater travels over the inlet weir and undergoes turbulent mixing before entering the wetland through a subsurface pipe. The brominated compounds such as bromodichloromethane, dibromochloromethane, and tribromomethane had 63−68% removal between the inlet splitter box and the IDZ. Tribromomethane concentrations were further reduced by 50% from the IDZ to the first deep zone (DZ1). Concentrations of benzene were reduced by 29%, chlorobenzene by 58%, and trichloromethane by 46% between the inlet splitter box and the IDZ. The inlet splitter box sample contained 12 additional VOC that were not measured in the other wetland samples: acetone (9.62 μg L^{-1}), 2-butanone (1.66 μg L^{-1}), bromochloromethane (0.31 μg L^{-1}), carbon disulfide (0.25 μg L^{-1}), dibromomethane (0.11 μg L^{-1}), chloromethane (0.22 μg L^{-1}), 4-methyl-2-pentanone (0.19 μg L^{-1}), 1,2,3-trichloropropane (0.06 μg L^{-1}), chloroethane (0.06 μg L^{-1}), 1,2,4-trichlorobenzene (0.04 μg L^{-1}), hexachloroethane (0.02 μg L^{-1}), and 1,4-isopropyltoluene (0.01 μg L^{-1}).

Volatilization Simulations. Volatilization is the primary removal mechanism for 1,4-dichlorobenzene, tetrachloroethene, dichloromethane, trichloromethane, bromodichloromethane, and dibromochloromethane in aquatic systems (44). Secondary removal pathways include reductive dechlorination, biodegradation, sorption, and plant uptake. Figure 3 shows results for inverse, two-film, and graphical volatilization simulations as well as measured concentrations for 1,4-dichlorobenzene, tetrachloroethene, bromodichloromethane, and toluene. The physical transport parameters were used in conjunction with $k_{vol,inverse}$, $k_{vol,2-film}$, and $k_{vol,graph}$ (Table 3) to simulate transport and first-order volatilization reactions.

Target VOC. Figure 3A,B shows excellent agreement with all three simulations and 1,4-dichlorobenzene and tetrachloroethene measured concentrations. The inverse simulation (67% removal) had the closest correspondence to measured concentrations (66% removal) for 1,4-dichlorobenzene. The two-film simulation slightly overestimated 1,4-dichlorobenzene removal (71%), and the graphical simulation underestimated removal (64%). At the ODZ, the tetrachloroethene inverse (70% removal), two-film (71% removal), and graphical (62% removal) simulations had good agreement with measured concentrations (65% removal). However, the tetrachloroethene measured outlet concentration does not decrease at the same rate as the other internally measured concentrations. Analysis of tetrachloroethene concentrations at the fifth deep zone (DZ5) indicated excellent agreement for the inverse (63% removal) and two-film (64% removal) simulations with measured concentra-
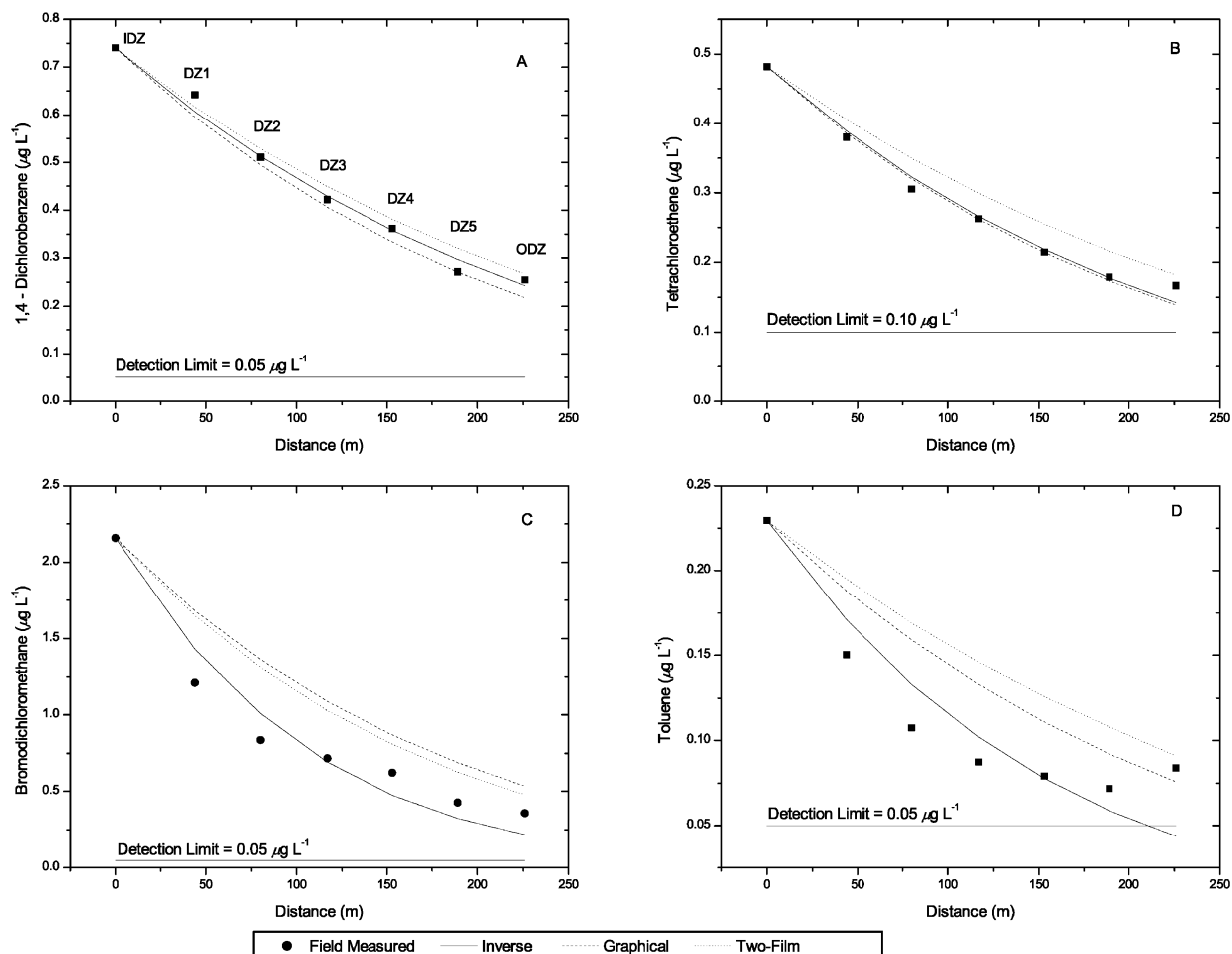
FIGURE 3. Field concentrations and volatilization simulations showing the inverse, two-film, and graphical approaches for (A) 1,4-dichlorobenzene, (B) tetrachloroethene, (C) bromodichloromethane, and (D) toluene (DZ = deep zone, I = inlet, O = outlet).

TABLE 3. Inverse ($k_{vol,inverse}$), Two-Film ($k_{vol,2-film}$), and Graphical ($k_{vol,graph}$) Volatilization Rates for VOC Detected in the Hayfield 1 Wetland

compound	$k_{vol,inverse}$ (s^{-1})	$k_{vol,2-film}$ (s^{-1})	$k_{vol,graph}$ (s^{-1})
Target VOC			
bromodichloromethane	9.40×10^{-6}	5.54×10^{-6}	5.99×10^{-6}
dibromochloromethane	1.21×10^{-5}	5.25×10^{-6}	6.53×10^{-6}
1,4-dichlorobenzene	4.42×10^{-6}	4.85×10^{-6}	4.05×10^{-6}
dichloromethane	4.62×10^{-6}	5.82×10^{-6}	3.46×10^{-6}
tetrachloroethene	4.81×10^{-6}	4.93×10^{-6}	3.88×10^{-6}
trichloromethane	4.63×10^{-6}	5.41×10^{-6}	3.67×10^{-6}
toluene	6.62×10^{-6}	4.41×10^{-6}	3.68×10^{-6}
Low-Level VOC			
benzene	1.64×10^{-6}	5.45×10^{-6}	1.69×10^{-6}
chlorobenzene	8.17×10^{-6}	5.11×10^{-6}	8.48×10^{-6}
diethyl ether	2.96×10^{-6}	5.16×10^{-6}	1.73×10^{-6}
ethylbenzene	1.19×10^{-6}	4.85×10^{-6}	9.61×10^{-7}
methyl-*tert*-butyl ether	1.67×10^{-6}	4.79×10^{-6}	2.08×10^{-6}
trichloroethene	4.24×10^{-6}	5.20×10^{-6}	3.04×10^{-6}
1,2-xylene	2.02×10^{-6}	4.84×10^{-6}	1.80×10^{-6}
1,3- + 1,4-xylene	9.43×10^{-7}	4.85×10^{-6}	1.03×10^{-6}

tions (63% removal), while the graphical simulation underestimated mass removal (55%).

The dichloromethane and trichloromethane measured concentrations demonstrated almost identical behavior, showing good agreement with all three simulations (data not shown). For both dichloromethane and trichloromethane, the inverse simulations (69% removal) had the best correla-

tion with field measurements (63% and 66% removal) at the ODZ. The two-film simulation overestimated mass removal for dichloromethane (77%) and trichloromethane (74%). In contrast, the graphical simulation underestimated mass removal for dichloromethane (58%) and trichloromethane (60%).

The measured concentrations of bromodichloromethane demonstrated faster removal between the IDZ and the second internal deep zone (DZ2), which was most closely replicated by the inverse simulation (Figure 3C). At DZ2, the inverse simulation (53% removal) had the closest correspondence with bromodichloromethane measured concentrations (61% removal), while the two-film (37% removal) and graphical (39% removal) simulation results deviated substantially from field measurements. At the ODZ, the variability between the methods was less, with the inverse (90% removal), two-film (75% removal), and graphical (78% removal) simulations having general agreement with measured concentrations (83% removal) for bromodichloromethane. In a similar manner, the dibromochloromethane simulation (data not shown) demonstrated better agreement at DZ2 between measured concentrations (70% removal) and the inverse simulation (62% removal), while the two-film (35% removal) and graphical (42% removal) simulations deviated significantly. At the ODZ, the inverse (95% removal), two-film (73% removal), and graphical (80% removal) simulations had general agreement with the measured concentrations (87% removal). The two-film and graphical simulations did not reproduce the observed initial drop in concentration, and the apparent agreement with outlet concentrations does not

accurately represent the internal behavior of the brominated compounds.

The toluene inverse simulation demonstrated agreement with internally measured concentrations (Figure 3D). At the fourth deep zone (DZ4), the inverse simulation (66% removal) had the best agreement with measured concentrations (65% removal), while the two-film (52% removal) and graphical (45% removal) simulations did not reproduce the rapid loss of toluene in the initial stages of the wetland. However, at the ODZ the measured concentrations (63% removal) had better agreement with the two-film (67% removal) and graphical simulations (60% removal) than the inverse simulation (81% removal). The graphical method closely corresponded to the outlet concentration without detailing the rapid mass loss internally observed in the wetland. The two-film simulation did not account for all of the internal removal observed in the wetland due to the assumption that volatilization is the principal removal pathway. Toluene may be susceptible to additional removal by biodegradation in aquatic systems (*44*).

Low-Level VOC. The low-level VOC inverse simulations demonstrated excellent agreement with field measurements, good agreement with graphical simulations, and generally deviated from the two-film simulations. The inverse simulations had very good agreement with field measurements at ODZ for benzene (inverse = 32% removal vs field measurement = 31% removal), methyl-*tert*-butyl ether (34% vs 40% removal), 1,2-xylene (39% vs 39% removal), and 1,3- + 1,4-xylene (17% vs 21% removal); at DZ5 for diethyl ether (45% vs 45% removal) and trichloroethene (58% vs 56% removal); and at DZ3 for chlorobenzene (63% vs 68% removal) and ethylbenzene (12% vs 14% removal). The two-film simulation results overestimated mass removals calculated from measured concentrations for benzene (two-film = 75% removal), methyl-*tert*-butyl ether (71% removal), 1,2-xylene (71% removal), and 1,3- + 1,4-xylene (71% removal) at ODZ; for diethyl ether (66% removal) and trichloroethene (66% removal) at DZ5; and ethylbenzene (45% removal) at DZ3, with the exception of chlorobenzene, which was lower (47% removal) at DZ3. The graphical simulations had good agreement with measured concentrations and overestimated removals for benzene (graphical = 34% removal) and methyl-*tert*-butyl ether (41% removal) at the ODZ; underestimated removals for 1,2-xylene (35% removal) and 1,3- + 1,4-xylene (19% removal) at the ODZ; and chlorobenzene (64% removal) and ethylbenzene (9% removal) at DZ3. However, the graphical simulations underestimated internal measured concentrations for diethyl ether (28% removal) and trichloroethene (46% removal) due to a higher ODZ concentration than measured in DZ5.

VOC Half-Life Calculations. *Target VOC.* The inverse, two-film, and graphical volatilization rates (Table 3) were converted to half-life values ($\ln(2)/k_{vol}$) to provide an estimate of relative residence time required for VOC removal via partitioning to the atmosphere (Figure 4). The inverse simulations include a 95% confidence interval for $k_{vol,inverse}$ that was converted to error bars for each VOC $t_{1/2,inverse}$. The total 95% confidence intervals for the $t_{1/2,inverse}$ simulations ranged from 6.7 to 11.9 h (16−49%) for target VOC with the exception of toluene (20.1 h, 70%). Published volatilization half-life values of 11−12 h for 1,4-dichlorobenzene (*44*), 0.3−0.5 h for tetrachloroethene (*45, 46*), 0.3−0.4 h for dichloromethane and trichloromethane (*45, 46*), and 5.2 h for toluene (*47*) significantly deviate from the wetland half-life calculations, likely due to the highly variable nature of surface and bulk agitation characteristics in laboratory studies versus the quiescent nature of flow regimes typical in wetland systems.

The $t_{1/2,2-film}$ values illustrate VOC partitioning behavior independent of wetland hydraulics (Figure 4). Similar
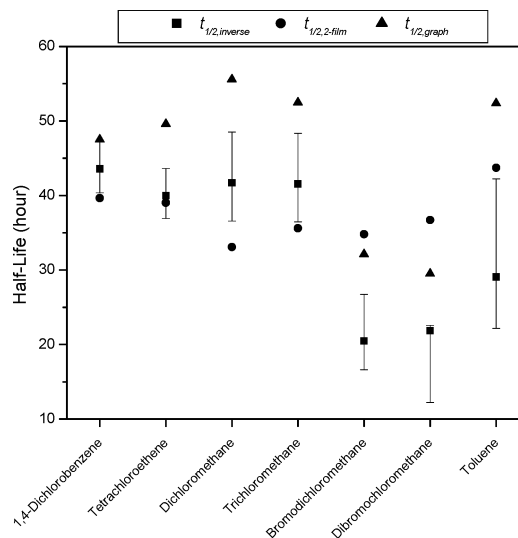

FIGURE 4. Half-life calculations for the inverse, two-film, and graphical approaches for 1,4-dichlorobenzene, tetrachloroethene, dichloromethane, trichloromethane, bromodichloromethane, dibromochloromethane, and toluene. Error bars represent 95% confidence interval for $t_{1/2,inverse}$.

compound composition resulted in $t_{1/2,2-film}$ values averaging 37.5 ± 3.6 h for target VOC and 38.0 ± 2.7 h for all VOC investigated. For 1,4-dichlorobenzene, tetrachloroethene, dichloromethane, and trichloromethane, the $t_{1/2,2-film}$ values ranged from 1 to 8.6 h (2−21%) shorter than $t_{1/2,inverse}$ values and 0.7−3.5 h (2−10%) from the lower 95% confidence limit. The $t_{1/2,2-film}$ values were longer than $t_{1/2,inverse}$ values by 14.3 h (70%) for bromodichloromethane, 14.8 h (68%) for dibromochloromethane, and 14.6 h (50%) for toluene and were 8.1 h (30%), 14.1 h (63%), and 1.5 h (3.4%) longer than the upper 95% confidence limit.

The $t_{1/2,graph}$ values represent a classical mathematical approach based on field concentrations and bulk hydraulic characterizations. The $t_{1/2,graph}$ values ranged from 3.9 to 13.9 h (9−33%) longer than $t_{1/2,inverse}$ values and from 0.2 to 7.1 h (0.4−14.6%) longer than the upper 95% confidence limit for 1,4-dichlorobenzene, tetrachloroethene, dichloromethane, and trichloromethane (Figure 4). The $t_{1/2,graph}$ values were longer than $t_{1/2,inverse}$ values for bromodichloromethane (57%) and dibromochloromethane (35%) and were 20% and 31% longer than the upper 95% confidence limit. For toluene, the $t_{1/2,graph}$ value was 80% longer than the $t_{1/2,inverse}$ value and 24% longer than the upper 95% confidence limit.

Low-Level VOC. The half-life calculations for the low-level compounds demonstrated similar trends to target VOC, with the $t_{1/2,inverse}$ half-life values generally longer than $t_{1/2,2-film}$ values and consistent with $t_{1/2,graph}$ values. The 95% confidence interval had good agreement with the associated $t_{1/2,inverse}$ values for trichloroethene (37%) and 1,2-xylene (17%) and lesser agreement for benzene (55%), chlorobenzene (66%), diethyl ether (71%), ethylbenzene (83%), and 1,3- + 1,4-xylene (94%). For methyl-*tert*-butyl ether, the 95% confidence interval (334.1 d) was the largest of any of the simulations ($t_{1/2,inverse}$ = 115.3 h,) due to field measurements that indicated overall removal (from IDZ to ODZ) but larger internal concentrations (DZ2, DZ3, DZ4) than observed at the inlet deep zone (IDZ). The $t_{1/2,2-film}$ values were less than the lower limit of the $t_{1/2,inverse}$ 95% confidence interval by 62% for benzene, 25% for diethyl ether, 67% for ethylbenzene, 31% for methyl-*tert*-butyl ether, 4% for trichloroethene, 55% for 1,2-xylene, and 73% for 1,3- + 1,4-xylene with the exception of chlorobenzene, which was 108% higher than the lower limit of the 95% confidence interval. The $t_{1/2,graph}$ values were lower than $t_{1/2,inverse}$ values by 3% for benzene, 4% for

chlorobenzene, 20% for methyl-*tert*-butyl ether, and 9% for 1,3- + 1,4-xylene. The $t_{1/2,\text{graph}}$ values were greater than $t_{1/2,\text{inverse}}$ values by 72% for diethyl ether, 24% for ethylbenzene, 40% for trichloroethene, and 12% for 1,2-xylene. Similar to target VOC, the published volatilization half-life values of 4.8 h for benzene (*47*), 9 h for chlorobenzene (*44*), 5−6 h for ethylbenzene (*44*), 0.3−0.4 h for trichloroethene (*45*, *46*), and 5.6 h for 1,2-xylene (*47*), are substantially shorter than observed in the wetland.

Discussion

Transport simulations using the inverse and two-film volatilization models illustrated good agreement for 1,4-dichlorobenzene, tetrachloroethene, dichloromethane, and trichloromethane; the inverse volatilization simulations had the best agreement with measured concentrations for all of the compounds. Bromodichloromethane, dibromochloromethane, and toluene underwent a substantial drop in concentration in the initial stages of the wetland that was not characterized by the two-film or graphical methods. This deviation suggests other processes influencing the brominated compound concentrations such as source variations. For example, WWTPs typically have diel variations in concentrations representing daily fluctuations in domestic and commercial activities, and the inlet sample may represent a time-dependent peak concentration that is greater than concentrations in the later deep zone samples where the daily concentration variations have been dampened by dispersion. Likewise, toluene was susceptible to additional removal pathways (biodegradation) not addressed by the two-film method. For the low-level compounds, the inverse and graphical simulation results had the best agreement with measured concentrations, while the two-film simulation results were generally substantially lower than outlet concentrations.

Overall, the inverse approach provided the most rigorous analysis of volatilization by including the effects of evaporation and groundwater infiltration on internal VOC levels. The mass removals calculated from the inverse simulations averaged 4% ± 7% higher than measured concentrations for all VOC investigated. It should be noted that the $k_{\text{vol,inverse}}$ values encompassed the rate of overall mass removal regardless of the specific removal pathway. The two-film method did not account for multiple removal pathways and therefore served as a general indicator of target VOC behavior. The mass removals calculated from the two-film simulations had better agreement with observed concentrations (averaging 6% ± 4% higher) for the chlorinated target VOC, than for the brominated compounds which averaged 11% ± 4% lower than measured concentrations. The graphical approach introduced error by not considering the effects of all of the hydrologic processes, specifically evaporation, on measured concentrations and resulted in generally good agreement with outlet concentrations and mass removal (3% ± 3%) and less agreement with internal removal characteristics. Although some of the simulations resulted in relatively large percent deviations from observed values, all OTIS model results were within 0.4 μg L^{-1} of measured concentrations.

Volatilization rates for compounds in the constructed wetland deviated substantially from published experimental values. The range of environmentally relevant removal rates emphasizes the importance of developing techniques to accurately quantify the transport and fate of contaminants in wastewater-dominated wetland systems. Difficulties arose in extrapolating laboratory results to wetland conditions due to the relatively low environmental concentrations (less than 10 μg L^{-1}) and the variable nature of surface and bulk agitation characteristics that ultimately determine volatilization rates.

Quiescent, slow-flow regimes prevailed in the constructed wetlands at the Tres Rios facility (velocities ranged from 3.89×10^{-4} to 1.10×10^{-3} m s^{-1}; *27*), which results in longer field half-life values than observed in laboratory experiments and more turbulent stream systems. In the wetland, the HRT (94 h) was nearly three times longer than the average target VOC $t_{1/2,\text{inverse}}$ value, allowing sufficient time for volatilization to occur and the resulting substantial reduction of environmental concentrations.

Theoretical models present a means of evaluating the importance of volatilization relative to other transport and fate processes but cannot be used as an absolute measure of volatilization rates from natural waters. For example, acetone (9.62 μg L^{-1}) and 2-butanone (1.66 μg L^{-1}) were detected at substantial concentrations in the inlet splitter box but were not target analytes in the wetland samples. Without the availability of additional field data, a two-film volatilization rate can be used in conjunction with hydraulic transport parameters to provide an order-of-magnitude estimation of compound residence time in the wetland. In this application, the two-film simulation for acetone had a 61% mass removal ($C_{\text{out}} = 3.79$ μg L^{-1}) with a $t_{1/2,2-\text{film}}$ value of 68.6 h, while the two-film simulation of 2-butanone had a mass removal of 62% ($C_{\text{out}} = 0.63$ μg L^{-1}) with a $t_{1/2,2-\text{film}}$ value of 66.0 h. The inverse and two-film simulation results as well as the $t_{1/2,\text{inverse}}$ and $t_{1/2,2-\text{film}}$ values had good agreement for chlorinated compounds and greater deviations for brominated compounds.

Several of the detected VOC (trichloromethane, bromodichloromethane, dibromochloromethane) are disinfection byproducts (DBP) formed when chlorine reacts with the dissolved organic carbon (DOC) in wastewater effluent (*17*, *48*). DOC produced internally by the wetland vegetation (*15*) was more reactive for production of DBP than DOC from the 91st Avenue WWTP (*49*). Water samples collected from the Hayfield wetland inlet in 1998 (*49*) had concentrations of trichloromethane, bromodichloromethane, dibromochloromethane, tetrachloroethene, tribromomethane, and trichloroethene that were within a factor of 2 of those reported in this study.

Constructed wetlands represent a complex system of interconnected physical, chemical, biological, and hydrodynamic processes that vary with time and space. Inherent difficulties arise by describing such complex systems using numerical analysis of explicit design equations. Overall, the model simulation results presented here demonstrate a suitable approach for investigating VOC removal in constructed wetlands. The use of tracer test results together with calculated and graphically determined volatilization rate coefficients illustrate investigative techniques using varying amounts of field measurements. Further analysis indicated that two-film volatilization rates may be used as a general indicator of VOC behavior in wetland systems in the absence of field data. The simulations presented here validate the application of stream modeling techniques to wetland systems.

Acknowledgments

Literature Cited

(1) Schulz, R.; Peall, S. K. C. *Environ. Sci. Technol.* **2001**, *35*, 422.

(2) Knight, R. L.; Kadlec, R. H.; Ohlendorf, H. M. *Environ. Sci. Technol.* **1999**, *33,* 973.

(3) Cole, S. *Environ. Sci. Technol.* **1998**, *32*, 218A.

(4) Sobolewski, A. *Ecol. Eng.* **1996**, *6*, 259.

(5) Kadlec, R. H.; Knight, R. L. *Treatment Wetlands*; Lewis Publishers: Boca Raton, FL, 1996; p 893.

(6) Knight, R. L. *Ecol. Eng.* **1992**, *1*, 97.

(7) Schwarzenbach, R. P.; Gschwend, P. M.; Imboden, D. M. *Environmental Organic Chemistry*; John Wiley & Sons: New York, 1993; p 681.

(8) Melcer, H. *Environ. Sci. Technol.* **1994**, *28*, 328A.

(9) Glaze, W. H.; Henderson, J. E. *J. Water Pollut. Control Fed.* **1975**, *47*, 2511.

(10) Gearhart, R. A.; Higley, M. In *Constructed Wetlands for Water Quality Improvement*; Moshiri, G. A., Ed.; Lewis Publishers: Boca Raton, FL, 1993; p 632.

(11) Kuehn, E.; Moore, J. A. In *Proceedings of the 4th International Conference on Wetlands Systems for Water Pollution Control*; ICWS '94 Secretariat: Guangzhou, China, 1994; p 732.

(12) Maynard, H. E.; Ouki, S. K.; Williams, S. C. *Water Res.* **1999**, *33*, 1.

(13) Sartoris, J. J.; Thullen, J. S.; Barber, L. B.; Salas, D. E. *Ecol. Eng.* **2000**, *14*, 49.

(14) Smith, L. K.; Sartoris, J. J.; Thullen, J. S.; Andersen, D. C. *Wetlands* **2000**, *20*, 684.

(15) Barber, L. B.; Leenheer, J. A.; Noyes, T. I.; Stiles, E. A. *Environ. Sci. Technol.* **2001**, *35*, 4805.

(16) Machate, T.; Heuermann, E.; Schramm, K.-W.; Kettrup, A. *J. Environ. Qual.* **1999**, *28*, 1665.

(17) Quanrud, D. M.; Karpiscak, M. M.; Lansey, K. E.; Arnold, R. G. *Water Sci. Technol.* **2001**, *44*, 267.

(18) Moore, B. J.; Ross, S. D.; Gibson, D.; Callow, L. In *Wetlands & Remediation: An International Conference, Salt Lake City, Utah, 1999*; Means, J. L.; Hinchee, R. E.; Eds.; Battelle Press: Columbus, OH, 2000; p 333.

(19) Kassenga, G. R.; Pardue, J. H.; Blair, S.; Ferraro, T. *Ecol. Eng.* **2003**, *19*, 305.

(20) Chen, S. C.; Zoltek, J. *Chemosphere* **1995**, *31*, 3455.

(21) Pardue, J. H. In *Wetlands & Remediation: An International Conference, Salt Lake City, Utah, 1999*; Means, J. L., Hinchee, R. E., Eds.; Battelle Press: Columbus, OH, 2000; p 301.

(22) Kadlec, R. H. *Water Sci. Technol.* **1997**, *35*, 149.

(23) Yahnke, J.; Stiles, E. *Tres Rios demonstration constructed wetlands project, project status and water quality data analysis report, phase 1, 1995 to 1998*; Bureau of Reclamation: Denver, CO, 2001; p 133.

(24) U.S. Environmental Protection Agency. *Free water surface wetlands for wastewater treatment, a technology assessment*; EPA-832-S-99-002; U.S. EPA, Office of Water: Washington, DC, 1999; p 151.

(25) Kadlec, R. H. *Ecol. Eng.* **2000**, *15*, 105.

(26) Buchberger, S. G.; Shaw, G. B. *Ecol. Eng.* **1995**, *4*, 249.

(27) Keefe, S. H.; Barber, L. B.; Runkel, R. L.; Ryan, J. N.; McKnight, D. M.; Wass, R. D. *Water Resour. Res.* **2004**, 40.

(28) Runkel, R. L. *Water Res. Invest.* (*U.S. Geol. Surv.*) **1998**, *No. 98-4018*, 73 (http://co.water.usgs.gov/otis).

(29) CH2M Hill. *Tres Rios demonstration constructed wetland project research Plan—First supplement*; CH2M Hill: Phoenix, AZ, 1997; p 1-1.

(30) Wass, Gerke and Associates, Inc. *Status report to the 1998 research plan for the Tres Rios demonstration constructed wetland project*; Wass, Gerke and Associates, Inc.: Phoenix, AZ, 2001; p 67.

(31) Connor, B. F.; Rose, D. L.; Noriega, M. C.; Murtagh, L. K.; Abney, S. R. *Open-File Rep.—U.S. Geol. Surv.* **1998**, *No. 97-829*, p 78.

(32) Fernald, A. G.; Wigington, P. J., Jr.; Landers, D. H. *Water Resour. Res.* **2001**, *37*, 1681.

(33) McKnight, D. M.; Kimball, B. A.; Runkel, R. L. *Hydrol. Proc.* **2001**, *15*, 1979.

(34) Runkel, R. L.; McKnight, D. M.; Andrews, E. D. *J. North Am. Benthic Soc.* **1998**, *17*, 143.

(35) Martinez, C. J.; Wise, W. R. *Ecol. Eng.* **2003**, *20*, 211.

(36) Lewis, W. K.; Whitman, W. G. *Ind. Eng. Chem.* **1924**, *16*, 1215.

(37) Rathbun, R. E. *U.S. Geol. Surv. Prof. Pap.* **1998**, *No. 1589*, 151.

(38) Chapra, S. C. *Surface water-quality modeling*; McGraw-Hill: Boston, MA, 1997; p 844.

(39) Lyman, W. J.; Reehl, W. F.; Rosenblatt, D. H. *Handbook of chemical property estimation methods—environmental behavior of organic compounds*; McGraw-Hill: New York, 1982; p 530.

(40) Howard, P. H.; Meylan, W. M. *Handbook of physical properties of organic chemicals*; Lewis Publishers: Boca Raton, FL, 1997; p 1585.

(41) Hayduk, W.; Laudie, H. *J. Am. Inst. Chem. Eng.* **1974**, *20*, 611.

(42) Fuller, E. N.; Schettler, P. D.; Giddings, J. C. *Ind. Eng. Chem.* **1966**, *58*, 19.

(43) Barber, L. B.; Keefe, S. H.; Brown, G. K.; Taylor, H. E.; Antweiler, R. C.; Peart, D. B.; Plowman, T. I.; Roth, D. A. *Water Resour. Invest.* (*U.S. Geol. Surv.*) **2003**, *No. 03-4129*, p 90.

(44) Callahan, M. A.; Slimak, M. W.; Gabel, N. W.; May, I. P.; Fowler, C. F.; Freed, J. R.; Jennings, P.; Durfee, R. L.; Whitmore, F. C.; Maestri, B.; Mabey, W. R.; Holt, B. R.; Gould, C. *Water-related environmental fate of 129 priority pollutants*; EPA-440/4-79-029b; U.S. EPA Office of Water: Washington, DC, 1979; p 39.

(45) Dilling, W. L.; Tefertiller, N. B.; Kallos, G. J. *Environ. Sci. Technol.* **1975**, *9*, 833.

(46) Dilling, W. L. *Environ. Sci. Technol.* **1977**, *11*, 405.

(47) Mackay, D.; Leinonen, P. J. *Environ. Sci. Technol.* **1975**, *9*, 1178.

(48) Rathbun, R. E. *Arch. Environ. Contam. Toxicol.* **1996**, *31*, 420.

(49) Rostad, C. E.; Martin, B. S.; Barber, L. B.; Leenheer, J. A.; Daniel, S. R. *Environ. Sci. Technol.* **2000**, *34*, 2703.